A study on the integration of air-source heat pumps, solar collectors, and PCM tanks for outdoor swimming pools for winter application in subtropical climates

Yantong Li[a], Natasa Nord[b], Huijun Wu[c], Zhun (Jerry) Yu[d], Gongsheng Huang[a,*]

[a]Department of Architecture and Civil Engineering, City University of Hong Kong, Tat Chee Avenue, Kowloon, Hong Kong, 999077, China

[b]Department of Energy and Process Engineering, Norwegian University of Science and Technology, Trondheim, 7049, Norway

[c]School of Civil Engineering, Guangzhou University, Guangzhou, 510006, China

[d]College of Civil Engineering, National Center for International Research Collaboration in Building Safety and Environment, Hunan University, Changsha, Hunan, 410082, China

*The corresponding author; Tele: 852-34422408; Fax: 852-34420427; Email: gongsheng.huang@cityu.edu.hk

ABSTRACT

This study presents a new integration of air-source heat pumps, solar collectors and PCM tank regarding the dynamics of outdoor swimming pools, and investigates its application in outdoor swimming pools for extending their availability in winter season for subtropical climates. The proposed integration system harvests heat from both ambient air via air-source heat pumps and solar radiation via solar collectors. PCM tank are introduced to shift the electricity use from the on-peak to off-peak period in order to reduce the operating cost. Since multiple heat sources are used, two issues in the development are addressed: 1) main components sizing and 2) multi-criterion design. The sizing problem is solved by considering the complementarity of different heating sources, while the multi-criterion design considers both the initial investment, thermal comfort, operating cost, and energy use. To illustrate the proposed main components sizing and multi-criterion design methods, a case study of using the heating system in a typical swimming pool in Hong Kong is conducted. Based on the proposed main component sizing method, the typical combinations of different solar collector area, air-source heat pump heating capacity, and PCM tank volume are determined using MATLAB codes. Based on the proposed multi-criterion design method, the results of the system operation simulated by TRNSYS and MATLAB in different cases are used to identify the optimal solar fraction. Thus, it can be

concluded that the proposed main components sizing, and multi-criterion design methods can well guide the design of the swimming pool heating system with multiple heat source.

Keywords: Air-source heat pump; Solar collector; PCM tank; Outdoor swimming pool; Multi-criterion design

1. Introduction

In subtropical climates outdoor swimming is a popular sport and there are thousands of outdoor swimming pools, which may be owned by governments, private properties, and hotels. However, most of them are closed during the entire winter season, normally from December to next April (Zsembinszki, Farid, and Cabeza 2012). This is because the outdoor weather condition during daytime in such a climate, cannot ensure the water temperature of the pool being maintained around 28^{o}C for thermal comfort. Consequently, there is a high heating demand, and if a conventional heating technology (e.g. using electrical or gas boiler) is used to fulfil this demand, the operating cost will be very high (Li, Ding, and Du 2020; Li et al. 2020).

For extending the availability of outdoor swimming pools in winter seasons, advanced heating systems have been developed. Some scholars conducted the investigations of using the solar collectors for heating outdoor swimming pools. For instance, Yadav and Tiwari (1987) analyzed the performance of the heating system using the solar collectors with heat exchangers. It was concluded that increasing the water flowrate and solar collector area could increase the water temperature. Rakopoulos and Vazeos (1987) used the experimental data to validate the reliability of an analytical model of the heating system with solar collectors. The similar work was conducted by Haaf et al. (1994). Molineaux (1994a) conducted the performance analysis of the system with solar collectors for heating five different swimming pools in Switzerland. The experimental study in the study of Croy and Peuser (1994) indicated that the heating system with solar collectors had a better economic performance than the conventional heating system. Dang (1986) concluded that the energy efficiency of solar collectors could reach up to 53.3% when they are used in a swimming pool of India. Some scholars conducted the investigations of using heat pumps for heating outdoor swimming pools. For instance, Greyvenstein and Meyer (1991) concluded that using heat pumps might be more economically beneficial than using solar collectors, because the initial cost of heat pumps might be lower than that of solar collectors. Lam and Chan (2003; 2001) used heat pumps to offer heat for a five-star hotel in Hong Kong, and it was concluded that the energy performance of the system was considerable in comparison with that of conventional heating systems. Some scholars conducted the investigations of using waste heat recovery technologies for heating outdoor swimming pools. For instance, Borge et al. (2011) concluded that using the waste heat from the air-conditioning systems could not only reduce the swimming pool heating demand, but also improve the energy efficiency of air-conditioning systems. Harrington and Modera (2013) found that the energy consumption of the air-condition system could be reduced by 25% to 30%

when its waste heat was offered to the swimming pool. Some scholars conducted the investigations of using geothermal energy technologies for heating outdoor swimming pools. For instance, Somwanshi et al. (2013) presented a simulation study for analyzing the performance of the system using geothermal plants, and they found that the pool water temperature could be maintained between 22^{o}C and 27^{o}C when the proposed system was used. Some scholars conducted the investigations of using biomass boilers for heating outdoor swimming pools. Katsaprakakis (2015) concluded that the operating cost of the system could be effectively reduced when the proposed system with biomass boilers were used.

Among these heating technologies, solar collectors and air-source heat pumps are most commonly used. The merit of solar collectors is their low energy use. However, the heat collected by solar collectors depends heavily on solar radiation intensity, which might suffer from stochastic changes and could not provide stable heat supply (Tian et al. 2018; Tian et al. 2019). Another issue is that a large area of solar collectors will be needed when they are used alone in subtropical climates as reported by Chow et al. (2012). Therefore, to reduce the solar collector area and increase the heat supply stability, solar collectors should be used together with other heating suppliers.

Compared with solar collectors, air-source heat pumps have the merit of availability at any time and can provide relatively stable heat supply (Yu et al. 2020; de Oliveira et al. 2015). They are suitable for applications under subtropical climates because the outdoor air temperature is usually above 10^{o}C during the whole winter, which can guarantee a good efficiency of heat collection. However, since air-source heat pumps need mechanical compressors that require electrical power input, higher energy use will be expected in comparison with solar collectors.

Therefore, it is meaningful to integrate air-source heat pumps and solar collectors to form a heating system and investigate its performance when it is used for outdoor swimming pools in winter. In addition, in the study of Li et al. (2018), phase change material (PCM) was used in a heating system, which stored heat collected from the air-source heat pumps and discharged it to the pool when heat is needed during the open period of the pool. Since the heat charge is scheduled to the electric off-peak period, the use of PCM can shift the electricity use of the air-source heat pumps from the on-peak to off-peak period to further reduce the operating cost. This study therefore proposes a heating system, which mainly consists of solar collectors, air-

source heat pumps, PCM tank as well as an insulation cover. Fig. 1 depicts the layout of the proposed heating system for outdoor swimming pool in winter. The heating system is designed corresponding to the 24-hours operation of a swimming pool (e.g. three stages including preheating, open, and close), and it works as follows:

- The solar collectors are used to collect heat from solar radiation and supply heat directly to the swimming pool.
- The air-source heat pumps have two purposes: one is to absorb heat from the ambient outdoor air and preheat the swimming pool before it is open for swimmers; another is to absorb heat and charge the PCM tank during the off-peak period.
- The PCM tank is used to provide heat when the heat from the solar collectors are not enough to maintain the water temperature of the pool within the thermal comfort range. It is charged by the air-source heat pumps during the off-peak period.
- The insulation cover is used to cover the swimming pool when it is closed in order to reduce the heat loss.

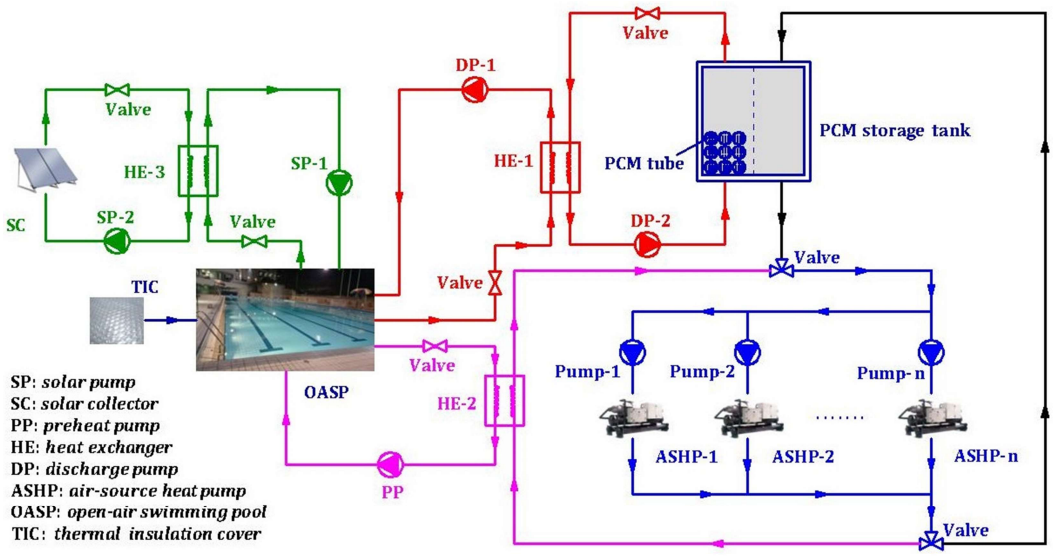

Fig. 1. Layout of proposed heating system for outdoor swimming pool in winter.

Although the integration of solar collectors, air-source heat pumps and PCM tank has been proposed, current studies mainly focused on its application in buildings (Plytaria et al. 2019). Considering the difference of the heating demand and operation modes between swimming pools and buildings, it is worthy to carry out a comprehensive investigation on the proposed heating system for outdoor swimming pools in subtropical climates for winter application. Two issues are addressed in this study: main components sizing and multi-criterion design. Unlike sizing a single heat source system, the sizing of a multiple heat source system is more

complicated, because the coupling among different heat sources needs to be considered. Since different contributions from different heat sources will affect the system performance, multi-criterion design is significant to understand and improve the overall performance of the proposed heating system.

The main contributions of this study are presented as follows: (a) the outdoor swimming pool heating system that considers multiple heat source is proposed and investigated; (b) the main components sizing method of the system is proposed, which can help engineers design the solar collector, air-source heat pumps, and PCM tank according to different solar fraction (γ); (c) the multi-criterion design method of the system is proposed, which can effectively identify the optimal γ according to the characteristics of the system, such as climates and swimming pool features; (d) the case study of applying the proposed system and methods in a typical swimming pool in Hong Kong effectively demonstrates their reliability.

The rest of the paper is organized as follows. Section 2 describes the proposed sizing approach considering the cooperation of different heat sources. Section 3 introduces the multi-criterion design strategy. Section 4 presents the case studies. Section 5 depicts the results and analysis. Concluding remarks are summarized in Section 6.

2. Main components sizing

2.1. Overview of the sizing method

The proposed sizing method is shown in Fig. 2. Firstly, the maximum daily heat energy demand, which is required for maintaining the water temperature of the pool at a design set point, is calculated under a selected weather condition (normally the worst-case weather condition) using a heat transfer model of the swimming pool without cover.

As two heat sources are used, it is necessary to allocate their individual contribution to fulfill the maximum daily heat energy demand. A design parameter (γ), called solar fraction, is therefore introduced to describe the percentage contribution from the solar collectors (Nord, Qvistgaard, and Cao 2016). Thus, the percentage contribution from the air-source heat pumps is denoted as $(1-\gamma)$. According to the heat energy contribution, the area of the solar collectors is estimated according to a predefined weather condition and rated operation schedule of the heating system. Since the heat contributed from air-source heat pumps will be completely

stored in the PCM tank, the volume of the PCM tank can be determined according to the thermal properties of the used PCM and configuration of the PCM tank.

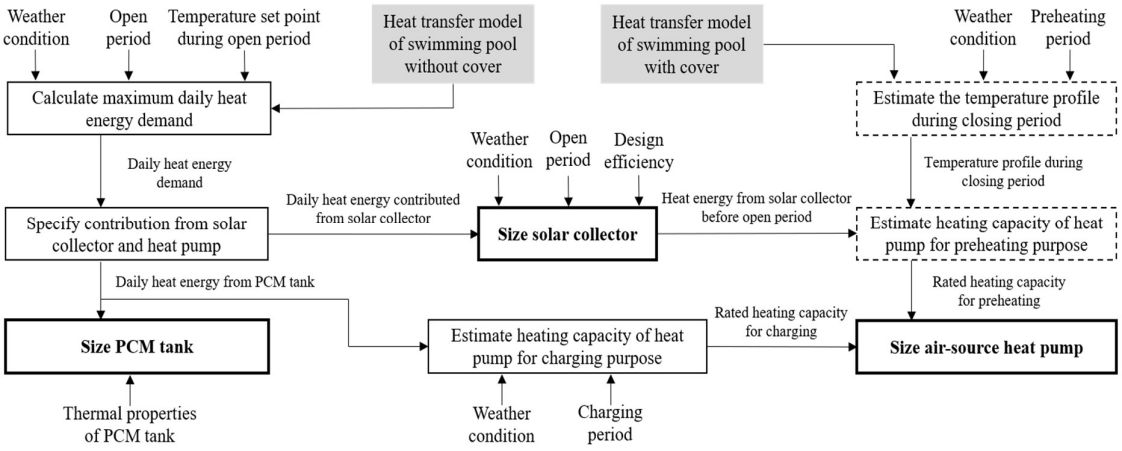

Fig. 2. Strategy for sizing main components, where necessary models are highlighted using grey boxes.

To determine the final rated heating capacity of the air-source heat pumps, it is needed to consider the rated heating capacity for charging the PCM tank and preheating the swimming pool. The heating capacity for charging is estimated according to the heat contribution from air-source heat pumps, a predefined weather condition, and the length of the charging period. The heating capacity for preheating is estimated using a heat transfer model of the swimming pool with the cover under a given weather condition, a predefined preheating period, and the water temperature profile of the swimming pool during the close period. The higher value among the heating capacity for charging and that for preheating is selected as the final rated heating capacity for air-source heat pumps.

As the rated operation schedule of the heating system is significant for the sizing, it should be specified before the sizing. Here, a general schedule in a 24-hour period is given in Table 1, where the important time instants are defined in Table 2, beginning from the electric off-peak use starting time (i.e. t_1). In Table 1, the PCM charging starts at the beginning of the off-peak period, which can reduce the rated power of the air-source heat pumps due to the availability of a longer charging period. It should be noted that:

- The PCM tank charging and the swimming pool preheating should be conducted during the off-peak period in order to reduce the electricity bill.
- When solar radiation is available, the solar collectors should start and supply heat to the

swimming pool directly. Before the swimming pool is open, the collected solar heat is used for preheating.

Table 1 The rated operation schedule of main components in a period of 24 hours

Time	$t_1 \rightarrow t_2$	$t_2 \rightarrow t_3$	$t_3 \rightarrow t_4$	$t_4 \rightarrow t_5$	$t_5 \rightarrow t_6$	$t_6 \rightarrow t_7$	$t_7 \rightarrow t_1$(next)
Pool	close				open		close
PCM tank	charge	idle			discharge		idle
Heat pump	on			off			
Solar collector	off		on			off	

Table 2 The important time instants in a period of 24 hours

Time instants	Actions
t_1	Off-peak electric use starts & PCM charging starts
t_2	Swimming pool preheating starts
t_3	Solar energy use starts
t_4	On-peak electric use starts
t_5	Swimming pool opens
t_6	Solar energy use stops
t_7	Swimming pool closes

2.2. Calculation for maximum daily heat energy demand

The maximum daily heat energy demand required for the swimming pool during the open period ($E_{m,open}$), is equal to the amount of the heat loss under the condition that the water temperature of the pool is maintained at the set point (T_{st}), which is calculated as:

$$E_{m,open} = \int_{t=t_5}^{t_7} q_{htr} dt \quad (1)$$

where q_{htr} (W) is the total heat transfer rate during the open period of the pool, which is given as (Buonomano et al. 2015):

$$q_{ht} = q_{sol,w} - (q_{eva} + q_{rad} + q_{conv} + q_{cond} + q_{rfs}) \quad (2)$$

where $q_{sol,w}$ (W) is the solar heat absorbed by the water of the pool; q_{eva} (W), q_{rad} (W), q_{conv} (W), and q_{cond} (W), and q_{rfs} (W) are the heat loss due to evaporation, radiation, convection, conduction, and refilling freshwater, respectively.

The solar heat absorbed by the swimming pool water ($q_{sol,w}$) is calculated as (Ruiz and Martínez 2010):

$$q_{sol,w} = A_{pool} \cdot \alpha_{sol} \cdot G_{sol} \tag{3}$$

where A_{pool} (m^2) is the surface area of the pool; α_{sol} ($-$) is the effective solar absorptance coefficient; and G_{sol} ($\mathrm{W/m}^2$) is the solar irradiance intensity.

The evaporative heat loss (q_{eva}) is calculated as:

$$q_{eva} = A_{pool} \cdot h_{eva} \cdot (p_{sat} - p_{amb}) \tag{4}$$

where h_{eva} ($\mathrm{W/(m^2 \cdot Pa)}$) is the evaporative heat transfer coefficient; p_{sat} (Pa) is the air saturated vapor pressure at the pool surface; and p_{amb} (Pa) is the air partial vapor pressure of the ambient temperature. According to the study in (Buonomano et al. 2015), they are given by:

$$h_{eva} = 0.0638 + 0.0669 \cdot v_{wind} \tag{5}$$

$$p_{sat} = 1000 \cdot 0.61121 \cdot e^{(18.678 - T_{st}/234.5) \cdot T_{st}/(257.14 + T_{st})} \tag{6}$$

$$P_{amb} = 1000 \cdot RH \cdot 0.61121 \cdot e^{(18.678 - T_{amb}/234.5) \cdot T_{amb}/(257.14 + T_{amb})} \tag{7}$$

where v_{wind} ($\mathrm{m/s}$) is the wind speed; T_{amb} (°C) is the ambient dry-bulb temperature; and RH ($-$) is the relative humidity.

The radiative heat loss (q_{rad}) is calculated by the Stefan- Boltzmann equation as (Ruiz and Martínez 2010; Zsembinszki, Farid, and Cabeza 2012):

$$q_{rad} = A_{pool} \cdot \varepsilon_{water} \cdot \sigma \cdot [(T_{st} + 273.15)^4 - (T_{sky} + 273.15)^4] \tag{8}$$

where ε_{water} ($-$) is the water emissivity coefficient; σ ($\mathrm{W/(m^2 \cdot K^4)}$) is the Stefan-Boltzmann constant; and T_{sky} is the equivalent sky temperature, given by (Harrington and Modera 2013; Woolley, Harrington, and Modera 2011):

$$T_{sky} = (T_{amb} + 273) \cdot \varepsilon_{sky}^{0.25} - 273.15 \tag{9}$$

where ε_{sky} ($-$) is the sky emissivity coefficient.

The convective heat loss (q_{cov}) is determined as:

$$q_{cov} = A_{pool} \cdot h_{cov} \cdot (T_{st} - T_{amb}) \tag{10}$$

where h_{cov} ($\mathrm{W/(m^2 \cdot K)}$) is the convective heat transfer coefficient between the pool surface and ambient environment, calculated as (Lam and Chan 2001):

$$h_{cov} = 2.8 + 3.0 \cdot v_{wind} \tag{11}$$

The conductive heat loss (q_{cond}) is determined as (Bergman and Incropera 2011):

$$q_{cond} = \frac{1}{2 \cdot L_{cod}} \cdot q_{dim} \cdot k_{soil} \cdot A_{cond} \cdot (T_{st} - T_{soil}) \quad (12)$$

where L_{cod} (m) is the characteristic length of the pool; q_{dim} $(-)$ is the dimensionless conductive heat transfer rate; k_{soil} $(\mathrm{W/(m \cdot K)})$ is the thermal conductivity of the soil; A_{cond} $(\mathrm{m^2})$ is the conductive heat transfer area of the pool; and T_{soil} (°C) is the soil temperature. Since the soil temperature is stable and could be considered as a constant, q_{cond} is considered as a constant in this study.

The heat loss caused by refilling freshwater into the swimming pool (q_{rfs}) is calculated by:

$$q_{rfs} = c_w \cdot \rho_w \cdot v_{rfs} \cdot (T_{st} - T_{rfs}) \quad (13)$$

where T_{rfs} (°C) is the temperature of the refilling fresh water, which is assumed to be 15°C (Buonomano et al. 2015); and v_{rfs} $(\mathrm{m^3/s})$ is the volumetric flow rate of the fresh water, which is assumed to be the 5% of the pool volume per day (Buonomano et al. 2015).

Note that in the above calculations, the weather parameters, including the solar irradiance intensity (G_{sol}), the wind speed (v_{wind}), the ambient dry-bulb temperature (T_{amb}), and the relative humidity (RH), should be from a worst-case weather condition, and thus the required daily heat energy amount is the maximum. More details on the worst-case weather condition will be given in the case studies.

2.3. Calculation for design area of solar collectors

As the heat amount contributed from the solar collectors is $\gamma \cdot E_{m,open}$, the design area of the solar collectors (A_{sc}) is estimated as:

$$A_{sc} = \frac{\gamma \cdot E_{m,open}}{\beta_{sc} \cdot E_{mt,des}} \quad (14)$$

where β_{sc} $(-)$ is the efficiency of the solar collectors; and $E_{mt,des}$ $(\mathrm{kWh/m^2})$ is the design value of the available solar energy intensity during the open period.

As the available solar energy intensity during the open period is highly stochastic, it might not be good to use the worst-case scenario. For example, Fig. 3 shows the distribution of the available solar energy intensity during the swimming pool open period (from 12:00 to 20:00) in a winter season (from December 1st to next April 30th) over ten years for Hong Kong (from

2003 to 2012), varying between 0.08 kWh/m^2 and 4.31 kWh/m^2. Among 1513 days, only 11 days have the intensity being not larger than 0.08 kWh/m^2. Hence, a probabilistic method is introduced to specify $E_{mt,des}$, shown as:

$$P\left(E_{mt} \le E_{mt,des}\right) \le \psi \tag{15}$$

where E_{mt} (kWh/m^2) is the potential available solar energy intensity during the open period; P $(-)$ indicates the cumulative probability; and ψ $(-)$ is a design parameter to assess the risk of the potential solar energy intensity being smaller than the design value. For example, if ψ is 50% (i.e. middle-level design risk), $E_{mt,des}$ will be 4.31 kWh/m^2.

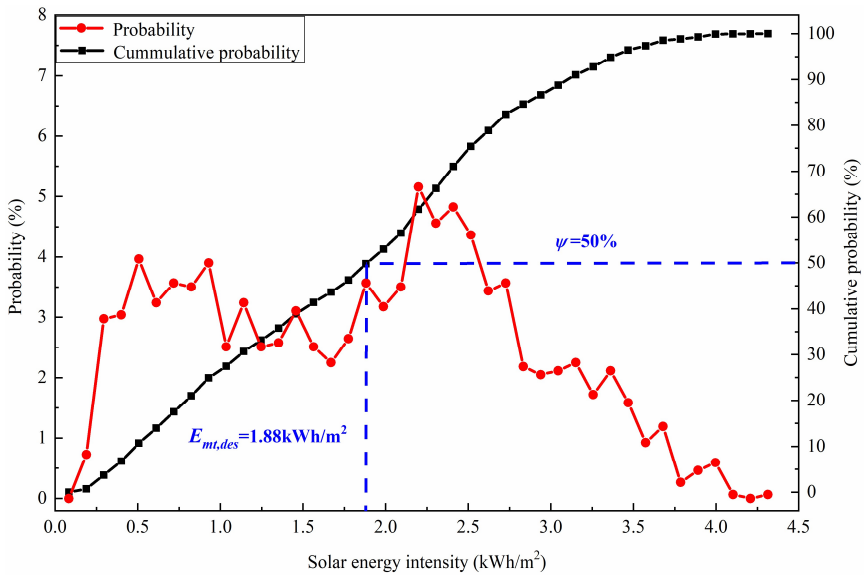

Fig. 3. Distribution of the available solar energy intensity during the swimming pool open period (from 12:00 to 20:00) and cumulative probability of the distribution.

2.4. Calculation for design volume of PCM tank

The heat energy amount that should be stored into the PCM tank is $(1-\gamma)\cdot E_{m,open}$. Because the tank temperature will be the same with the water temperature of the pool (at the set point, T_{st}) after releasing all the stored heat to the pool, the design volume of PCM tank (V_{pst}) is given by (Pirasaci and Goswami 2016):

$$V_{pst} = \frac{(1-\gamma)\cdot E_{m,open}}{(1-\eta_w)\cdot\rho_p\cdot\left[cp_s\cdot(T_m-T_{st})+cp_l\cdot(T_{tank,d}-T_m)\right]+\eta_w\cdot c_w\cdot\rho_w\cdot(T_{tank,d}-T_{st})+(1-\eta_w)\cdot\rho_p\cdot H_p} \tag{16}$$

where η_w $(-)$ is the water fraction; $T_{tank,d}$ (°C) is the design temperature after fully charged; cp_s (kJ/kg · K) and cp_l (kJ/kg · K) are the solid and liquid specific heat of the PCM, respectively; c_w (kJ/kg · K) is the specific heat of the water; ρ_p (kg/m^3) and ρ_w (kg/m^3) are

the density of the PCM and water in the storage tank, respectively; and H_p (kJ/kg) is the latent heat of the PCM.

2.5. Calculation for design rated heating capacity of air-source heat pumps

2.5.1. Rated heating capacity for charging

The heat energy amount that should be stored into the PCM tank ($(1-\gamma)\cdot E_{m,open}$) is also used to estimate the rated heating capacity of the heat pumps, because the heat pumps are used to charge the PCM tank. The rated heating capacity for charging ($q_{hp,ch}$) is given by:

$$q_{hp,ch} = \frac{(1-\gamma)\cdot E_{m,open}}{t_2 - t_1} \tag{17}$$

Note that in this calculation the heat delivered from the heat pumps to the PCM tank is assumed to be a constant during the charging period. As shown in Table 1, PCM tank is charged by air-source heat pumps during the period ($t_1 \rightarrow t_2$), and thus the design charging time is equal to be ($t_2 - t_1$).

2.5.2. Rated heating capacity for preheating

To estimate the rated heating capacity for preheating, the temperature drop (Δ_u marked in Fig. 4 (a)) from the moment of closing the pool (t_7) to the moment of starting the preheating (t_2) needs to be estimated. Meanwhile, the required temperature rise (Δ_l marked in Fig. 4 (a)) that guarantees that the water temperature, should reach the temperature set point (T_{st}) at the beginning of the opening needs to be estimated as well.

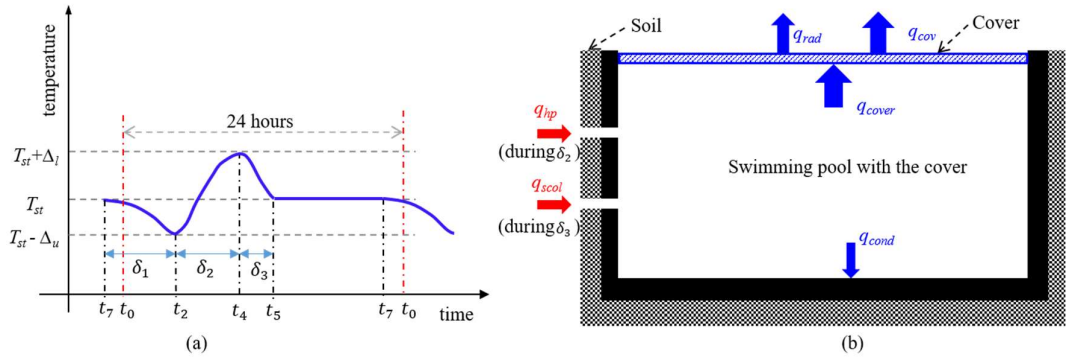

Fig. 4. (a) Rated water temperature profile of the pool; and (b) heat transfer model of the pool with cover.

To facilitate the calculation, δ_1, δ_2, and δ_3 are used to denote the length of the period from t_7 to t_2, from t_2 to t_4, and from t_4 to t_5 as shown in Fig. 4 (a), respectively. The first step is to calculate Δ_u and Δ_l. Afterwards, the rated heating capacity of the heat pumps for preheating could be estimated according to Δ_u and Δ_l.

2.5.2.1. Calculation of Δ_u during the period of δ_1

During this period, it is assumed that the ambient temperature (T_{amb}) and the sky temperature (T_{sky}) are stable. The heat loss of the pool with the cover ($q_{loss,c}$) satisfies the following as (Harrington and Modera 2013):

$$q_{loss,c} = q_{rad} + q_{conv} \tag{18}$$

where q_{rad} (W) is the radiative heat loss from the cover; and q_{conv} (W) is the convective heat loss from the cover. They are given by:

$$q_{rad} = A_{pool} h_{rad} (T_{c,up} - T_{sky}) \tag{19}$$

$$q_{conv} = A_{pool} h_{conv} (T_{c,up} - T_{amb}) \tag{20}$$

where h_{rad} ($\mathrm{W/m^2 \cdot K}$) is the cover radiative heat transfer coefficient; h_{conv} ($\mathrm{W/m^2 \cdot K}$) is the cover convective heat transfer coefficient; and $T_{c,up}$ (°C) is the temperature of the cover upper surface (the surface towards the sky).

As the cover lower surface contacted with the water of the pool, its temperature is considered as the same with the water temperature of the pool. Thus, the heat flux from the water of the pool to the cover (q_{cover}) is:

$$q_{cover} = A_{pool} h_{cover} (T_{pool} - T_{c,up}) \tag{21}$$

where h_{cover} ($\mathrm{W/m^2 \cdot K}$) is the heat transfer coefficient due to the thermal conduction of the cover. Since $q_{loss,c}$ is equal to q_{cover} as well, i.e. $q_{cover} = q_{rad} + q_{conv}$, the cover upper surface temperature ($T_{c,up}$) is given by:

$$T_{c,up} = d_1 T_{pool} + d_2 T_{sky} + d_3 T_{amb} \tag{22}$$

where

$$d_1 = \frac{h_{cover}}{h_{cover}+h_{rad}+h_{conv}},\ d_2 = \frac{h_{rad}}{h_{cover}+h_{rad}+h_{conv}},\ d_3 = \frac{h_{conv}}{h_{cover}+h_{rad}+h_{conv}} \tag{23}$$

As shown in Fig. 4 (b), during the period of δ_1, the water temperature of the pool satisfies:

$$\rho_w c_w V_{pool} \frac{dT_{pool}}{dt} = -q_{cover} - q_{cond} \tag{24}$$

where q_{cond} (W) is the heat loss of the pool through its sidewalls and floor given by Eqn. (12).

According to Eqns. (21), (22) and (12), Eqn. (24) can be reformulated as:

$$\frac{dT_{pool}}{dt} = \alpha_1 T_{pool} + \alpha_2 T_{sky} + \alpha_3 T_{amb} + \alpha_4 T_{soil} \tag{25}$$

where α_1 $(1/s)$, α_2 $(1/s)$, α_3 $(1/s)$, and α_4 $(1/s)$ are the coefficients, given by:

$$\alpha_1 = -\left[h_{cover} A_{pool}(1-d_1) + \frac{1}{2L_{cond}} q_d k_{soil} A_{cond}\right] / \left(\rho_w c_w V_{pool}\right) \tag{26}$$

$$\alpha_2 = \frac{h_{cover} A_{pool} d_2}{\rho_w c_w V_{pool}},\ \alpha_3 = \frac{h_{cover} A_{pool} d_3}{\rho_w c_w V_{pool}},\ \alpha_4 = \frac{1}{2\rho_w c_w V_{pool} L_{cond}} q_d k_{soil} A_{cond} \tag{27}$$

When T_{sky}, T_{amb} and T_{soil} are considered stable during this period, Eqn. (25) becomes:

$$\frac{dT_{pool}}{dt} = \alpha_1 T_{pool} + C_1 \tag{28}$$

where $C_1 = \alpha_2 T_{sky} + \alpha_3 T_{amb} + \alpha_4 T_{soil}$. Thus, the water temperature of the pool (T_{pool}) is:

$$T_{pool} = \frac{D_1}{\alpha_1} e^{\alpha_1 t} - \frac{C_1}{\alpha_1} \tag{29}$$

where D_1 is a constant. At the beginning of the period δ_1 $(t = 0)$, the T_{pool} is T_{st}, and at the end of the period δ_1 $(t = \delta_1)$, the T_{pool} is $T_{st} - \Delta_u$. Thus,

$$T_{st} = \frac{D_1}{\alpha_1} - \frac{C_1}{\alpha_1};\ T_{st} - \Delta_u = \frac{D_1}{\alpha_1} e^{\alpha_1 \delta_1} - \frac{C_1}{\alpha_1} \tag{30}$$

which gives the temperature drop from the moment of closing the pool (t_7) to the moment of starting the preheating (t_2) (Δ_u) as:

$$\Delta_u = \frac{D_1}{\alpha_1}\left(1 - e^{\alpha_1 \delta_1}\right)\ with\ D_1 = \alpha_1 T_{st} + C_1 \tag{31}$$

2.5.2.2. Calculation of Δ_l during the period of δ_3

During the period of δ_3, the ambient temperature (T_{amb}) and the sky temperature (T_{sky}) are considered as constants. Note that during this period the solar collectors might be able to supply heat to the swimming pool. Thus, the water temperature of the pool satisfies:

$$\rho_w c_w V_{pool} \frac{dT_{pool}}{dt} = q_{scol} - q_{cover} - q_{cond} \tag{32}$$

where q_{scol} (W) is the heat gain by solar collectors during the period of δ_3.

$$q_{scol} = \frac{\beta_{sc} \cdot E_{mx,des} \cdot A_{sc}}{t_5 - t_4} \tag{33}$$

where $E_{mx,des}(\mathrm{kWh/m^2})$ is the design value of the available solar energy intensity during the period of δ_3, which is identified using the probabilistic method presented in Eqn. (15). Similarly, Eqn. (32) is reformatted as:

$$\frac{dT_{pool}}{dt} = \alpha_1 T_{pool} + C_3 + \frac{q_{scol}}{\rho_w c_w V_{pool}} \tag{34}$$

which has the following solution:

$$T_{pool} = \frac{D_3}{\alpha_1} e^{\alpha_1 t} - \frac{C_3}{\alpha_1} - \frac{q_{scol}}{\alpha_1 \rho_w c_w V_{pool}} \tag{35}$$

At the beginning of the period δ_3 ($t = 0$), the T_{pool} should be $T_{st} + \Delta_l$, and at the end of the period ($t = \delta_3$), the T_{pool} should be T_{st}. Thus,

$$T_{st} + \Delta_l = \frac{D_3}{\alpha_1} - \frac{C_3}{\alpha_1} - \frac{q_{scol}}{\alpha_1 \rho_w c_w V_{pool}} \tag{36}$$

$$T_{st} = \frac{D_3}{\alpha_1} e^{\alpha_1 \delta_3} - \frac{C_3}{\alpha_1} - \frac{q_{scol}}{\alpha_1 \rho_w c_w V_{pool}} \tag{37}$$

which gives

$$\Delta_l = \frac{D_3}{\alpha_1}\left(1 - e^{\alpha_1 \delta_3}\right),\ D_3 = \left(\alpha_1 T_{st} + C_3 + \frac{q_{scol}}{\rho_w c_w V_{pool}}\right) e^{-\alpha_1 \delta_3} \tag{38}$$

2.5.2.3. Estimation of rated heating capacity during the period of δ_2

When the heat pumps are used to preheat the pool water during the period of δ_2, the water temperature of the pool satisfies:

$$\rho_w c_w V_{pool} \frac{dT_{pool}}{dt} = q_{hp,pr} - q_{cover} - q_{cond} \tag{39}$$

where $q_{hp,pr}$ (W) is the rated heating capacity for preheating. When T_{sky}, T_{amb} and T_{soil} are considered as constants during this period, Eqn. (39) is reformulated as:

$$\frac{dT_{pool}}{dt} = \alpha_1 T_{pool} + C_2 + \frac{q_{hp,pr}}{\rho_w c_w V_{pool}} \tag{40}$$

The solution of Eqn. (40) is:

$$T_{pool} = \frac{D_2}{\alpha_1} e^{\alpha_1 t} - \frac{C_2}{\alpha_1} - \frac{q_{hp,pr}}{\alpha_1 \rho_w c_w V_{pool}} \tag{41}$$

At the beginning of the period δ_2 ($t = 0$), the T_{pool} should be $T_{st} - \Delta_u$, and at the end of the period ($t = \delta_2$), the T_{pool} should be $T_{st} + \Delta_l$. Thus,

$$T_{st} - \Delta_u = \frac{D_2}{\alpha_1} - \frac{C_2}{\alpha_1} - \frac{q_{hp,pr}}{\alpha_1 \rho_w c_w V_{pool}} \tag{42}$$

$$T_{st} + \Delta_l = \frac{D_2}{\alpha_1} e^{\alpha_1 \delta_2} - \frac{C_2}{\alpha_1} - \frac{q_{hp,pr}}{\alpha_1 \rho_w c_w V_{pool}} \tag{43}$$

Thus, the rated heating capacity for preheating ($q_{hp,pr}$) is given by:

$$q_{hp,pr} = \frac{\rho_w c_w V_{pool}\left[(\alpha_1 T_{st} - \alpha_1 \Delta_u + C_2) e^{\alpha_1 \delta_2} - (\alpha_1 T_{st} + \alpha_1 \Delta_l + C_2)\right]}{1 - e^{\alpha_1 \delta_2}} \tag{44}$$

2.5.3. Rated heating capacity of air-source heat pumps

As discussed previously, the final rated heating capacity of the heat pumps ($q_{hp,r}$) is the larger one between $q_{hp,ch}$ and $q_{hp,pr}$, which is therefore specified by:

$$q_{hp,r} = \max\left(q_{hp,ch}, q_{hp,pr}\right) \tag{45}$$

where $q_{hp,ch}$ and $q_{hp,pr}$ are given by Eqns. (17) and (44), respectively.

3. Multi-criterion design

As presented in the sizing strategy in Section 2, the design parameter (γ) impacts the performance of the heating system regarding initial cost, total operating cost, thermal comfort, and total energy use. Hence, it is necessary to investigate how it affects these performance indices. Fig. 5 gives the methodology to carry out this investigation. The first step is to specify a number of values for γ. For each value, the main components including the air-source heat pumps, PCM tank, and solar collectors, are sized using the method introduced in Section 2. Afterwards, the performance of the heating system is simulated on a platform. Some models in a system platform cannot be simulated by single software, and thus multiple software are integrated to establish the platform. In this study, this platform is constructed using the software TRNSYS and MATLAB, where TRNSYS is used to simulate the behaviors of the air-source heat pumps, water pumps, and controllers, etc.; while MATLAB is used to simulate the swimming pool and PCM tank. With the generated data, the performance indices are analyzed, based on which a suitable design can be selected.

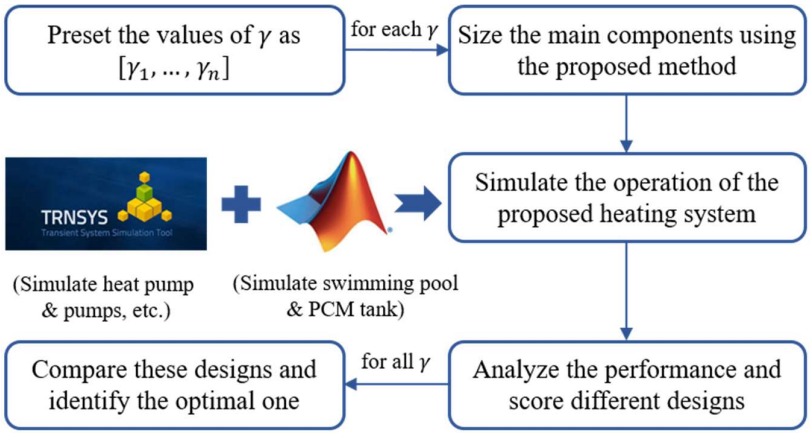

Fig. 5. Methodology for proposed multi-criterion design.

The performance indices, including thermal comfort, total energy use, initial cost, and total operating cost, are introduced and defined as follows. The thermal comfort is evaluated using

the thermal comfort unmet percentage (TU), which is defined as the total thermal comfort unmet hours divided by the total hours of the open period during the entire winter:

$$TU = \frac{1}{t_{tot}} \int_0^{t_{tot}} TC_{um} dt \tag{46}$$

where t_{tot} (s) denotes the total open hours of the pool during the entire winter; and TC_{um} $(-)$ is an indicator given by:

$$TC_{um} = \begin{cases} 0, \text{if } T_{pool} \geq T_{st} - \Delta_{st} \\ 1, \text{if } T_{pool} < T_{st} - \Delta_{st} \end{cases} \tag{47}$$

where Δ_{st} (°C) is a user-defined threshold for the thermal comfort.

The initial cost (IC) is calculated as:

$$IC = IC_{sc} + IC_{pst} + IC_{ashp} + IC_{oth} \tag{48}$$

where IC_{sc} (US$), IC_{pst} (US$), IC_{ashp} (US$), and IC_{oth} (US$) are the initial cost of the solar collectors, PCM tank, air-source heat pumps, and other components, respectively.

The total operating cost in a winter season (OC), consisted of the cost for the electricity use during the on-peak and off-peak period, is calculated as:

$$OC = OC_{d,onpk} + OC_{d,ofpk} + OC_{e,onpk} + OC_{e,ofpk} \tag{49}$$

where $onpk$ and $ofpk$ denote the on-peak and off-peak period, respectively; and d and e denote the demand and energy charge, respectively.

The total energy use in a winter season (EC), including the energy consumption of the air-source heat pumps and water pumps, is calculated as:

$$EC = E_{hp} + E_{wp} \tag{50}$$

where E_{hp} (kWh) and E_{wp} (kWh) denote the energy consumption of the air-source heat pumps and water pumps, respectively.

To weight the performance in a fare manner, the performance indices are normalized by:

$$S_{TU} = \frac{TU - TU_{lp}}{TU_{mp} - TU_{lp}}, S_{IC} = \frac{IC - IC_{lp}}{IC_{mp} - IC_{lp}}, S_{OC} = \frac{OC - OC_{lp}}{OC_{mp} - OC_{lp}}, S_{EC} = \frac{EC - EC_{lp}}{EC_{mp} - EC_{lp}} \tag{51}$$

where S_{TU} (-), S_{IC} (-), S_{OC} (-), and S_{EC} (-) are the normalized thermal comfort unmet percentage, initial cost, total operating cost, and total energy use, respectively; and lp and mp denote the least and most preferred performance, respectively. The overall performance score (S_{OP}) is given by:

$$S_{OP} = \tau_{tu} \cdot S_{TU} + \tau_{ic} \cdot S_{IC} + \tau_{oc} \cdot S_{OC} + \tau_{ec} \cdot S_{EC} \quad (52)$$

where τ_{tu} (-), τ_{ic} (-), τ_{oc} (-), and τ_{ec} (-) are the weighting factor, being user-specified and satisfying:

$$\tau_{tu} + \tau_{ic} + \tau_{oc} + \tau_{ec} = 1 \quad (53)$$

To compare with a conventional heating system, the total CO_2 emission (CE) is used to evaluate the environmental impact of the heating system, which is calculated as:

$$CE = EC \cdot e_c \quad (54)$$

where e_c is the CO_2 emissions factor for electricity, which is set as 0.756 ton/MWh (Shirazi, Taylor, et al. 2016).

4. Case studies

The outdoor swimming pool considered in this study is located at the City University of Hong Kong. The swimming pool has a total volume of 1,963.5 m^3. Its length and width are 50 m and 22 m, respectively. The depth varies from 1.2 m to 2.5 m (in the middle) with the average of 1.785 m.

4.1. Rated operation schedule

To size the main components, the rated operation schedule of the heating system was specified. Table 3 lists the significant time periods in a 24-hour operation schedule. The charging of the PCM tank was started at 21:00 (t_1), the beginning of the electric off-peak period; and it was completed at 05:00 (t_2), the beginning of the preheating for the pool. The preheating was completed at 09:00 (t_4), the beginning of the electric on-peak period. The solar energy available period was from 06:00 (t_3) to 18:00 (t_6). The swimming pool open from 12:00 (t_5) to 20:00 (t_7).

Table 3 Significant time periods in this study

Time periods	Values
$t_1 \rightarrow t_2$	21:00 – 05:00
$t_2 \rightarrow t_3$	05:00 – 06:00
$t_3 \rightarrow t_4$	06:00 – 09:00
$t_4 \rightarrow t_5$	09:00 – 12:00
$t_5 \rightarrow t_6$	12:00 – 18:00

$t_6 \rightarrow t_7$	18:00 – 20:00
$t_7 \rightarrow t_1$	20:00 – 21:00

4.2. Simulation platform

The simulation platform of the system was constructed using TRNSYS and MATLAB. Type 941 was adapted for the air-source heat pumps with the rated COP of 5.5. Type 3b was used for the model of the pumps. Type 91 was selected as the heat exchanger, where the effectiveness of the heat exchanger was assumed to be 0.95. Type 649 and Type 647 were utilized for the mixing and diverting valves, respectively. The PID controller for controlling the water temperature of the pool was simulated by Type 23. Type 71 was used to simulate the evacuated tube solar collectors. The heat transfer models of the outdoor swimming pool and the PCM tank were solved by MATLAB codes. They were linked into TRNSYS 17 by the MATLAB interface Type 155. The model of the outdoor swimming pool utilized in the simulation platform was identical with the model described in the sizing process in Section 2.2. The model of PCM tank and its structure was presented in the studies of Li et al. (2020). Paraffin wax was selected as PCM in this study and its thermal parameters were given in Table 4 (Hasan, Basher, and Shdhan 2018).

Table 4 Thermal properties of paraffin wax (Hasan, Basher, and Shdhan 2018)

Name of parameters	Symbol	Unit	Value
Phase change temperature	T_m	°C	44
Latent heat of PCM	H_p	kJ/kg	174.12
Solid specific heat of PCM	cp_s	kJ/(kg·K)	2.44
Liquid specific heat of PCM	cp_l	kJ/(kg·K)	2.53
Solid Density of PCM	ρ_s	kg/m^3	830
Liquid density of PCM	ρ_l	kg/m^3	783
Thermal conductivity	k_p	W/(m·K)	0.13

4.3. Information for calculating maximum daily heat energy demand

To calculate the maximum daily thermal energy demand of the pool during the open period ($E_{m,open}$), the meteorological data in a design day was utilized. The ten-winter meteorological data of Hong Kong from December 1st to April 30th, from 2003 to 2012, bought from Hong Kong Observatory, were analyzed, shown in Fig. 6. It can be seen that the average dry-bulb

temperature in winter season was around 19 ºC; the average wet-bulb temperature was around 16 ºC; the average wind speed was around 2.3m/s; and the average solar irrandance (from 06:00 to 18:00) is around 256W/m^2. After analyzing the ten-winter meteorological data, February 26th, 2005 was selected as the design day. The dry-bulb temperature, wet-bulb temperature, wind speed, and solar irradiance in this day were given in Fig. 6. Table 5 shows the parameters that were used for calculating the $E_{m,open}$. Under these conditions, the maximum heat energy demand was calculated as 14,444 kWh.

Table 5 Parameters used for calculating maximum daily heat energy

Name of parameters	Symbol	Unit	Value
Effective solar absorptance coefficient of the water	$\alpha_{sol,w}$	-	0.85
Emissivity coefficient of the water	ε_w	-	0.95
Dimensionless conduction heat transfer rate	q_{dim}		0.943
Thermal conductivity of the soil	k_{soil}	W/(m·K)	0.52
Emissivity coefficient of the sky	ε_{sky}	-	0.95
Design water temperature of the pool	T_{st}	ºC	28
Soil temperature	T_{soil}	ºC	17

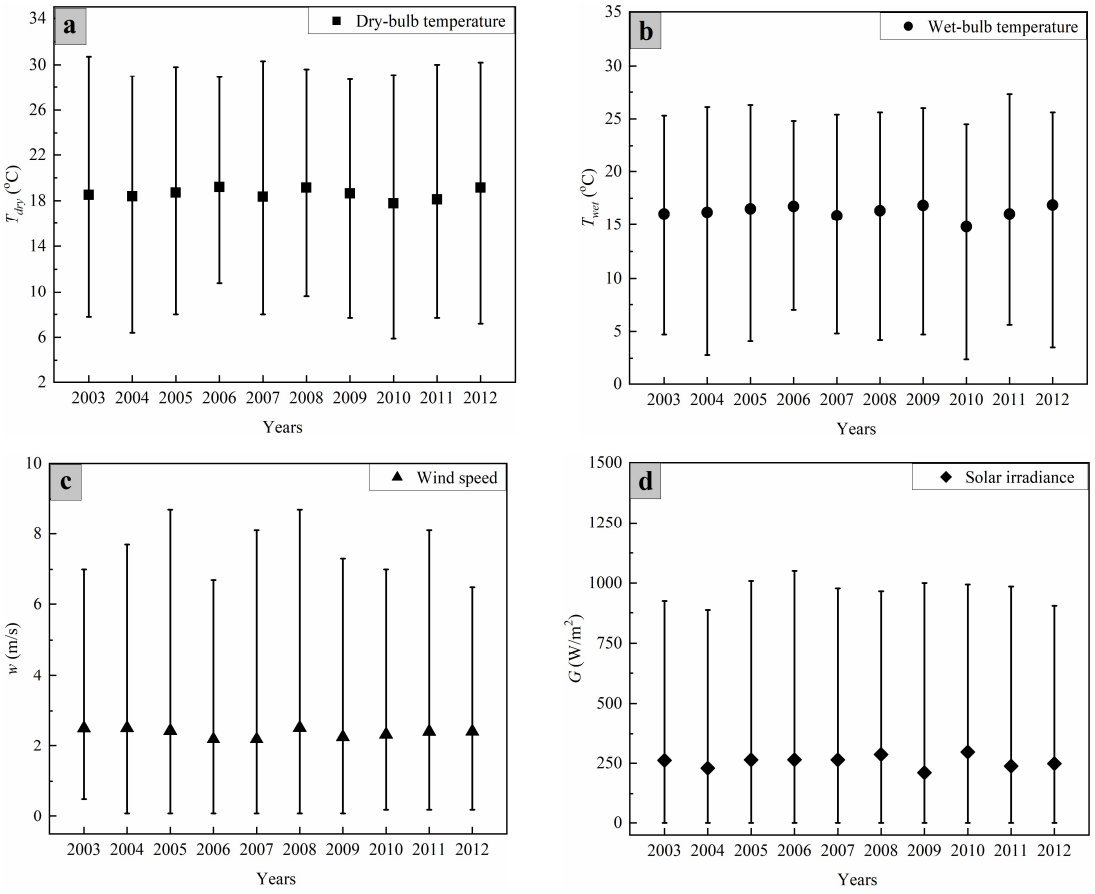

Fig. 6. Average hourly (a) dry-bulb tempearture; (b) wet-bulb temperature; (c) wind speed; and (d) solar irradiance in winter seasons from 2003 to 2012.

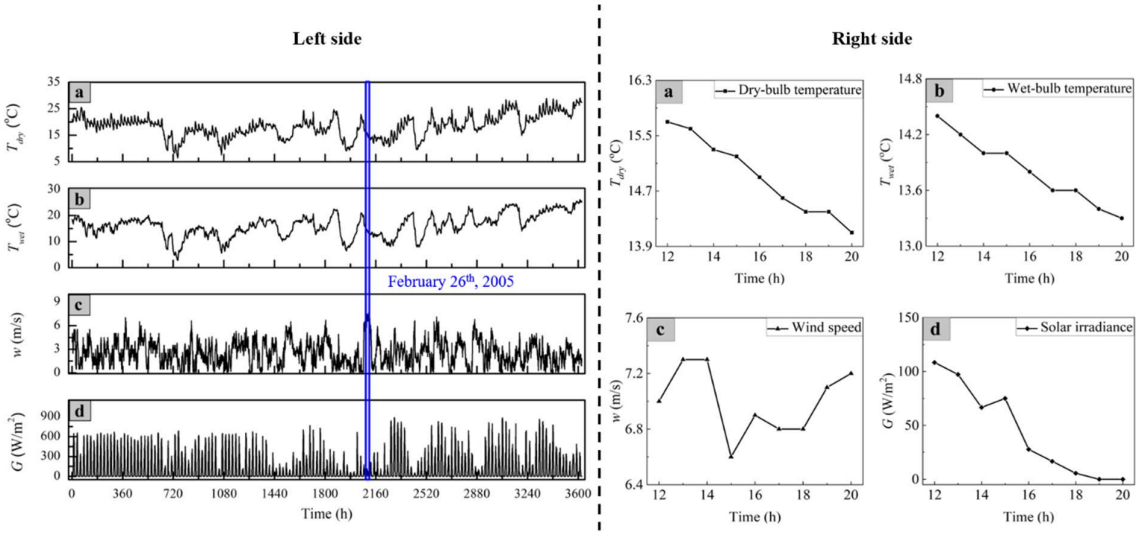

Fig. 7. Meteorological data (for sizing) containing: (a) dry-bulb temperature; (b) wet-bulb temperature; (c) wind speed; and (d) solar irradiance. (Left side: from December 1st, 2004 to April 30th, 2005; and right side: from 12:00 to 20:00 in February 26th, 2005)

4.4. Information for sizing area of solar collectors

During the sizing process of solar collectors, the efficiency of the solar collectors (β_{sc}), was set as 0.687 (Shirazi, Taylor, et al. 2016). A middle-level design risk shown in Fig. 2 was used to identify the design value of the available solar energy intensity during the open period ($E_{mt,des}$). When the cumulative probability (ψ) was 50% (i.e. middle-level risk), the $E_{mt,des}$ was 1.88 kWh/m^2. Given the heat energy contributed from the solar collectors ($\gamma \cdot E_{m,open}$), the total area of the solar collector was calculated using Eqn. (14).

4.5. Information for sizing volume of PCM tank

The rest of the maximum daily heat energy demand ($(1-\gamma) \cdot E_{m,open}$), was utilized to calculate the volume of the PCM tank using Eqn. (16). The design temperature of the PCM tank after fully charged ($T_{tank,d}$), i.e. maximum design water temperature that air-source heat pumps can reach, was set as 60 ^{o}C (Vieira, Stewart, and Beal 2015); and the water fraction of the PCM tank (η_w) was set as 0.25. Table 4 presented the thermal parameters of the used PCM.

4.6. Information for sizing heating capacity of air-source heat pumps

The $(1-\gamma) \cdot E_{m,open}$ was also utilized to estimate the heating capacity of air-source heat pumps for charging the PCM tank using Eqn. (17). Meanwhile, the heating capacity of air-source heat pumps for preheating was estimated according to the temperature profile during the closed period. The thickness of the cover was set to be 1 mm (Sonnier et al. 2015), and its thermal properties were given in Table 6. To identify the design value of the available solar energy intensity during the period of δ_3 (from 9:00 to 12:00) ($E_{mx,des}$) in Eqn. (33), the solar energy intensity during this period was analyzed. Fig. 8 showed the distribution of the available solar energy intensity during the period of δ_3 (from 9:00 to 12:00) in a winter season (from December 1st to next April 30th) over ten years for Hong Kong (from 2003 to 2012), varying between 0.07 kWh/m^2 and 3.55 kWh/m^2. A middle-level risk was used in this study, which suggested that the cumulative probability (ψ) was 50%. Thus, the $E_{mt,des}$ was 1.38 kWh/m^2. The ambient temperature for the period of δ_1, δ_2, and δ_3 were set as 6.0^{o}C, 5.9^{o}C, and 6.9^{o}C, respectively.

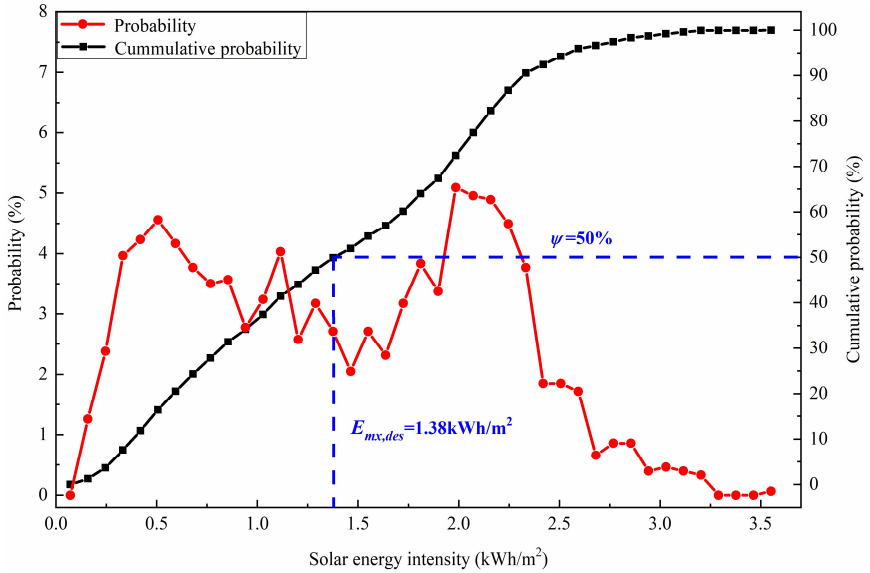

Fig. 8. Distribution of the available solar energy intensity during the period of δ_3 (from 9:00 to 12:00) and cumulative probability of the distribution.

Table 6 Thermal properties of the cover

Name of parameters	Symbol	Unit	Value
Radiative heat transfer coefficient of the cover	h_{rad}	W/(m^2·K)	4.6
Convective heat transfer coefficient of the cover	h_{conv}	W/(m^2·K)	10
Thermal conductivity of the cover	k_{cond}	W/(m·K)	0.36

5. Results and analysis

5.1. Model validation

The tested data in Shirazi et al. (2016) were used to validate the solar collector model; and the experimental data in Watanabe et al. (1993) and Ruiz et al. (2010) were used to validate the swimming pool and the PCM tank model, respectively. To describe the accuracy of the models, the average relative error (γ_a) between the simulated and experimental results was used, defined by:

$$\gamma_a = \frac{1}{s}\sum_{k=1}^{k=s}\left|\frac{y_{exp,k}-y_{sim,k}}{y_{exp,k}}\right| \times 100\% \quad (55)$$

where s is the number of experiment samples; and $y_{exp,k}$ and $y_{sim,k}$ are the experimental and simulated values, respectively.

The values of the parameters and work conditions utilized in the simulation were set as the same with the tested/experimental environment in the literatures. Fig. 9 showed the comparison between the simulated and tested/experimental results of the solar collector, swimming pool, and PCM tank, respectively. The γ_a for the solar collector, swimming pool, and PCM tank model were 0.20%, 0.65%, and 3.97%, respectively. Hence, the accuracy of the solar collector, swimming pool, and PCM tank model were believed to be acceptable.

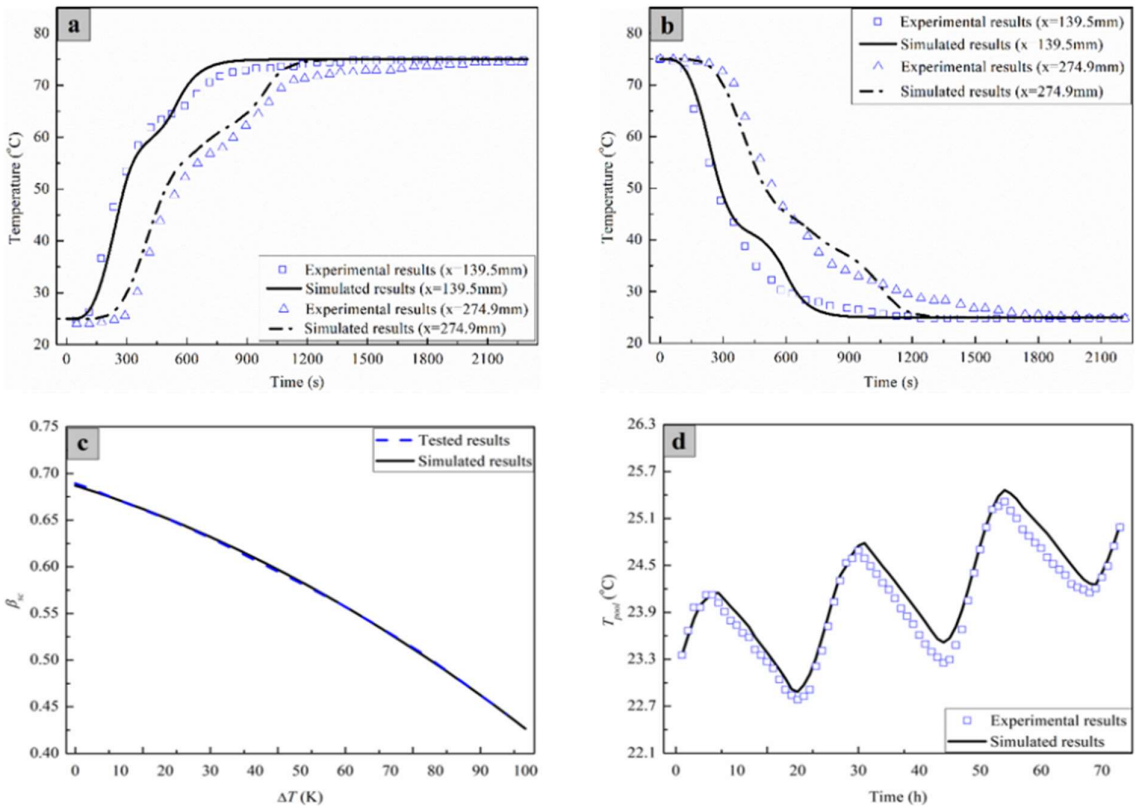

Fig. 9. Comparison between the tested/experimental and simulated results for: (a) charging process of PCM tank model; (b) discharging process of PCM tank model; (c) solar collector model, where ΔT is the temperature difference between the water and ambient environment; and (d) swimming pool model.

5.2. Main components sizing results

Table 7 shows the sizing results for different γ. Note that if only the solar collector was used, i.e. $\gamma = 100\%$, then the A_{sc} could reach 9,598.2 m^2, which was more than four times of the swimming pool surface area. However, it might be hard to find enough space to install the solar collectors with the A_{sc} of 9,598.2 m^2 in practice, especially in crowed cities like Hong Kong. Thus, in this study the indicator (ε_{sp}) was proposed to deal with this issue, shown as follows:

$$\varepsilon_{sp} = \frac{A_{sc}}{A_{pool}} \tag{56}$$

The statistical results from the literatures were used to identify the maximum ε_{sp} for maximizing the A_{sc}. Table 8 presents the statistical results of A_{sc}, A_{pool}, and ε_{sp} in the literatures. Fig. 10 shows a diagram to present the statistical results of ε_{sp}. It can be seen that the maximum ε_{sp} is 3.33, which is identified from the studies of Buonomano et al. (2015). According to the Eqn. (55), the maximum A_{sc} is 3,663 m^2. Correspondingly, according to the Eqn. (14), the maximum γ is 32.8%. Thus, the ranges of γ are from 0% to 32.8%. In this study, it is divided into 21 cases, and the difference of γ between the neighboring cases is nearly 1.6%.

Table 7 Sizing results of proposed heating system

γ (%)	A_{sc} (m^2)	q_{hp} (kW)	V_{pst} (m^3)	γ (%)	A_{sc} (m^2)	q_{hp} (kW)	V_{pst} (m^3)	γ (%)	A_{sc} (m^2)	q_{hp} (kW)	V_{pst} (m^3)
0	0	1,805.0	278.0	11.5	1,282.1	1,598.0	246.1	22.9	2,564.1	1,390.9	214.2
1.6	183.2	1,775.4	273.4	13.1	1,465.2	1,568.4	241.5	24.6	2,747.3	1,361.3	209.6
3.3	366.3	1,745.8	268.8	14.7	1,648.4	1,538.8	237.0	26.2	2,930.4	1,331.8	205.1
4.9	549.5	1,716.3	264.3	16.4	1,831.5	1,509.2	232.4	27.9	3,113.6	1,302.2	200.5
6.6	732.6	1,686.7	259.7	18.0	2,014.7	1,479.6	227.9	29.5	3,296.7	1,272.6	196.0
8.2	915.8	1,657.1	255.2	19.7	2,197.8	1,450.1	223.3	31.1	3,479.9	1,243.0	191.4
9.8	1,098.9	1,627.5	250.6	21.3	2,381.0	1,420.5	218.7	32.8	3,663.0	1,213.4	186.9

Table 8 Statistical results of A_{sc}, A_{pool}, and ε_{sp} in the literatures

Literatures	A_{sc}(m^2)	A_{pool}(m^2)	ε_{sp} (-)	Literatures	A_{sc}(m^2)	A_{pool}(m^2)	ε_{sp} (-)
Alkami and Sherif (1992)	300	1,172	0.26	Buonomano et al. (2015)	1,700	600	2.83
Alkami and Sherif (1992)	400	1,172	0.34	Buonomano et al. (2015)	1,800	600	3
Alkami and Sherif (1992)	500	1,172	0.43	Buonomano et al. (2015)	1,900	600	3.17
Alkami and Sherif (1992)	600	1,172	0.51	Buonomano et al. (2015)	2,000	600	3.33
Alkami and Sherif (1992)	700	1,172	0.6	Chow et al. (2012)	100	1,507	0.07
Alkami and Sherif (1992)	800	1,172	0.68	Chow et al. (2012)	250	1,507	0.17
Alkami and Sherif (1992)	900	1,172	0.77	Chow et al. (2012)	500	1,507	0.33
Alkami and Sherif (1992)	1,000	1,172	0.85	Chow et al. (2012)	750	1,507	0.5
Alkami and Sherif (1992)	1,100	1,172	0.94	Chow et al. (2012)	1,000	1,507	0.66
Alkami and Sherif (1992)	1,200	1,172	1.02	Chow et al. (2012)	1,200	1,507	0.8
Brambley and Wells (1983)	112	112	1	Chow et al. (2012)	1,400	1,507	0.93
Buonomano et al. (2015)	100	600	0.17	Croy and Peuser (1994)	-	-	0.5 - 0.8
Buonomano et al. (2015)	200	600	0.33	Dang (1986)	376	275	1.37

Buonomano et al. (2015)	300	600	0.5	Govaer (1984)	200	373	0.54
Buonomano et al. (2015)	400	600	0.67	Hahne and Kubler (1994)	1,359	2,433	0.56
Buonomano et al. (2015)	500	600	0.83	Hahne and Kubler (1994)	649.6	1,200	0.54
Buonomano et al. (2015)	600	600	1	Hahne and Kubler (1994)	500	1,050	0.48
Buonomano et al. (2015)	700	600	1.17	Molineaux et al. (1994a; 1994b)	412	1,320	0.31
Buonomano et al. (2015)	800	600	1.33	Molineaux et al. (1994a; 1994b)	888	2,200	0.4
Buonomano et al. (2015)	900	600	1.5	Molineaux et al. (1994a; 1994b)	625	1,360	0.46
Buonomano et al. (2015)	1,000	600	1.67	Molineaux et al. (1994a; 1994b)	266	1,250	0.21
Buonomano et al. (2015)	1,100	600	1.83	Molineaux et al. (1994a; 1994b)	745	3,140	0.23
Buonomano et al. (2015)	1,200	600	2	Rakopoulos and Vazeos (1987)	780	1,100	0.71
Buonomano et al. (2015)	1,300	600	2.17	Ruiz and Martinez (2010)	25	50	0.5
Buonomano et al. (2015)	1,400	600	2.33	Ruiz and Martinez (2010)	50	50	1
Buonomano et al. (2015)	1,500	600	2.5	Zhao et al. (2018)	20.5	36	0.57
Buonomano et al. (2015)	1,600	600	2.67				

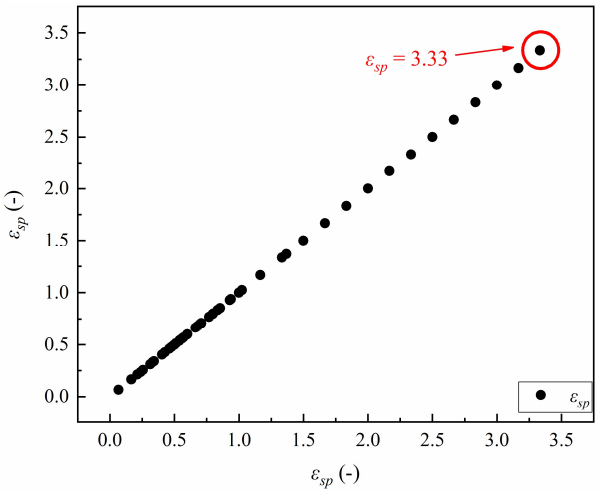

Fig. 10. Statistical results of ε_{sp}.

5.3. Performance evaluation

To investigate the influence of γ on the performance of the system, the simulations were run for each design candidate. Ten-winter weather data (from 2003 to 2012) were considered. Fig. 11 (a) shows the variation of the IC with different γ. The initial costs of main components were given in Table 9, where the prices were set according to the current market in Hong Kong. It was found that IC linearly increased with the increase of γ. This was due to the high unit cost of the solar collectors. The maximum value was US$658,501 when γ was 32.8%; while the minimum value was US$401,542 when γ was 0%, which was 39% of the maximum.

Table 9 Unit costs of main components in the proposed system

Name of components	Unit	Cost (US$/unit)
PCM tank	m^3	316
Air-source heat pump	kW	165
Solar collector	m^2	104
Insulation cover	m^2	4
Heat exchanger	-	780
Pump	-	663
Controller	-	3,331

Fig. 11 (b) shows the TU with different γ. It was found that all the values of TU in different γ were lower than 0.125%, which meant that the thermal comfortable requirement in the considered cases could be satisfied. However, there was still a trend that the higher γ led to the higher TU due to the stochastic solar radiation intensity. When $\gamma = 32.8\%$ ten-winter average TU reached its maximum value of 0.013%; while ten-winter average TU become 0% when γ was less than 21.3%.

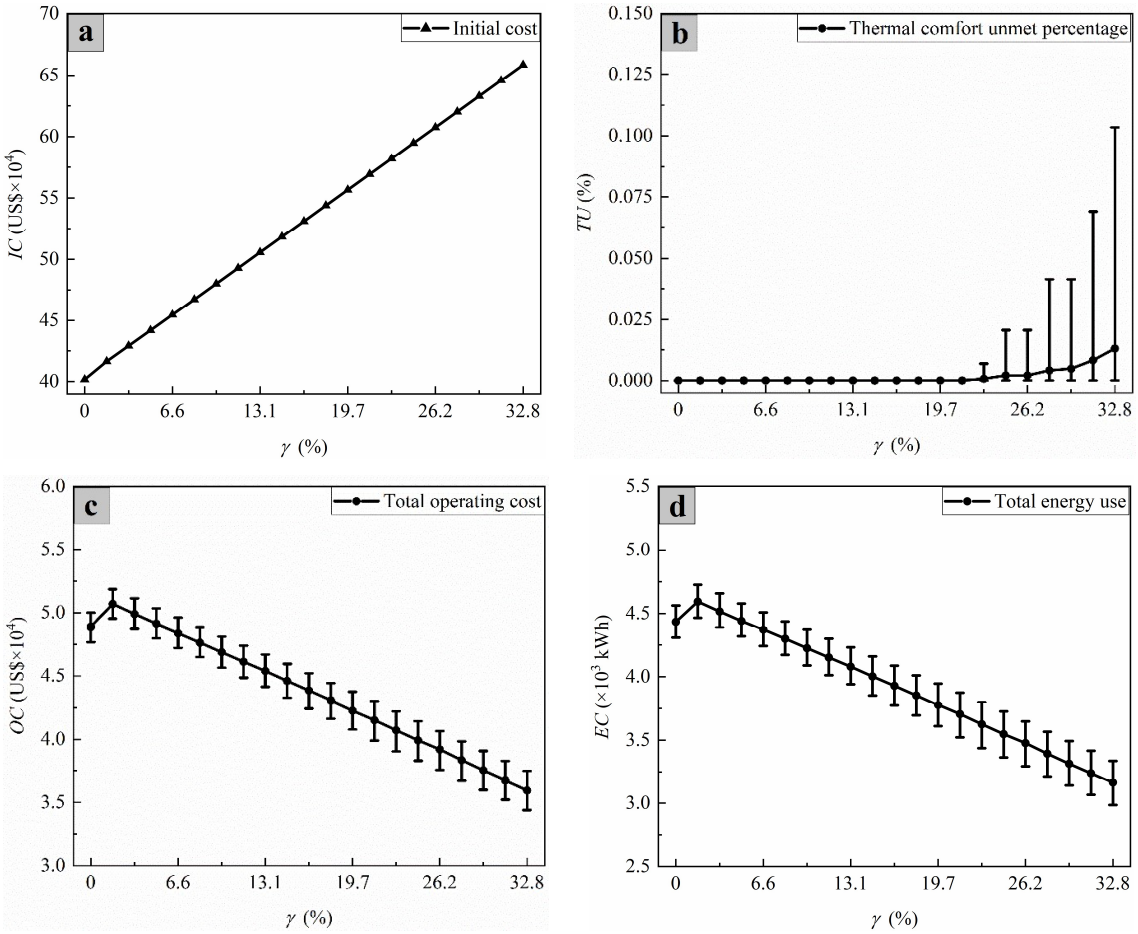

Fig. 11. Variations of (a) IC; (b) TU; (c) OC; and (d) EC. (Note: symbol for a given γ denoted ten-winter average value; and upper and lower bars denoted minimum and maximum value, respectively.)

Fig. 11 (c) shows the variation of the OC with different γ. The information for calculating the OC in Eqn. (49) was presented in the study of Li et al. (Li et al. 2020). It was found that in general, when more solar collectors were used, the OC became lower. This was reasonable because solar collectors collected heat with very low energy use. The maximum OC was US$48,879 (US$32 for each day), occurring when $\gamma = 0\%$. The minimum OC was US$35,958 (US$24 for each day), occurring when $\gamma = 32.8\%$, which was 29% of the maximum.

Fig. 11 (d) shows the variation of the EC with different γ. It was found that in general, more energy was used when the γ was lower, because the increasing energy consumed by the associated pumps of solar collectors was lower than the decreasing energy consumed by air-source heat pumps for charging. The maximum EC was 448,468 kWh, occurring when $\gamma =$

0%. The minimum EC was 314,673 kWh, occurring when $\gamma = 32.8\%$, which was 27% of the maximum.

5.4. Multi-criterion design results

Fig. 11 already demonstrated that γ had a significant influence on the performance of the system, which also indicated the necessity of the multi-criterion design. In addition, different combinations of weighting factors had an important effect on the S_{OP}. Table 10 shows the typical combinations of different weighting factors. Five typical combinations of different weighting factors were considered in this study, and the τ_{tu}: τ_{ec}: τ_{oc}: τ_{ic} were 1:1:1:2, 1:1:2:1, 1:2:1:1, 2:1:1:1, and 1:1:1:1, respectively. Fig. 12 shows the variation of S_{OP} with different γ. The optimal γ in the Cases 1, 2, 3, 4, and 5 was 0%, 29.5%, 29.5%, 21.3%, and 26.2%, respectively. The corresponding optimal combinations of A_{sc}, q_{hp}, and V_{pst} in the optimal γ were shown in Table 10.

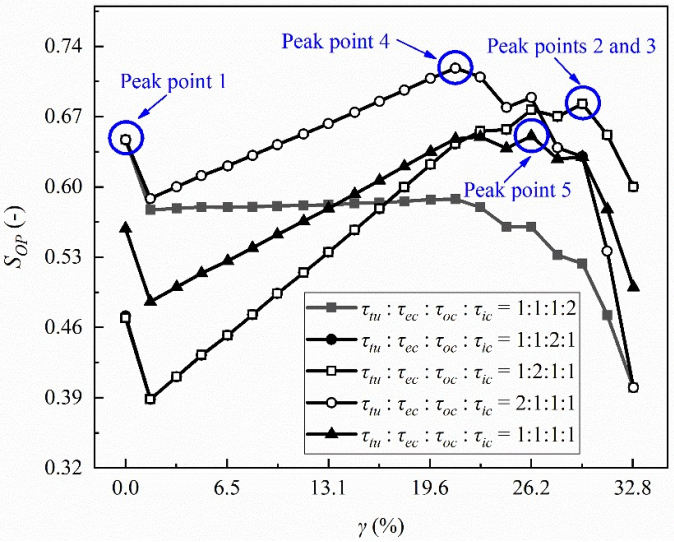

Fig. 12. Variation of S_{OP} with different γ.

Table 10 Typical combinations of different weighting factors and corresponding optimal variables

Cases	τ_{tu}	τ_{ec}	τ_{oc}	τ_{ic}	τ_{tu}: τ_{ec}: τ_{oc}: τ_{ic}	γ (%)	A_{sc} (m^2)	q_{hp} (kW)	V_{pst} (m^3)
1	0.2	0.2	0.2	0.4	1:1:1:2	0	0	601.7	278.0
2	0.2	0.2	0.4	0.2	1:1:2:1	29.5	3296.7	424.2	196.0
3	0.2	0.4	0.2	0.2	1:2:1:1	29.5	3296.7	424.2	196.0

4	0.4	0.2	0.2	0.2	2:1:1:1	21.3	2381.0	473.5	218.7
5	0.25	0.25	0.25	0.25	1:1:1:1	26.2	2930.4	443.9	205.1

The optimal design in the peak point 4 ($\gamma = 26.2\%$) was considered as an example to compare the CO_2 emission of the conventional and proposed heating system. In this case, the daily average operating cost was US$27. The ten-winter average EC was 363,593kWh, and the corresponding CO_2 emission was 274.9 ton. For the comparison, the ten-winter average EC of a conventional electrical heating system was 1,111,111 kWh, and the corresponding CO_2 emission was 840.0 ton. Hence, the CO_2 emission reduction could be as high as 67.3%.

To clearly present the water temperature variation of the pool, Fig. 13, as an example, showed the weekly water temperature variation of the pool from December 9th, 2006 to December 15th, 2006. During the open period, the water temperature could be maintained around 28°C by the PI controller. The water temperature would decrease after the preheating period when the heat from the solar collectors was not enough to overcome the heat loss, such as during December 9th and 13th. The water temperature would increase before the open period, because heat collected by the solar collector was directly input into the swimming pool, such as December 11th and 12th.

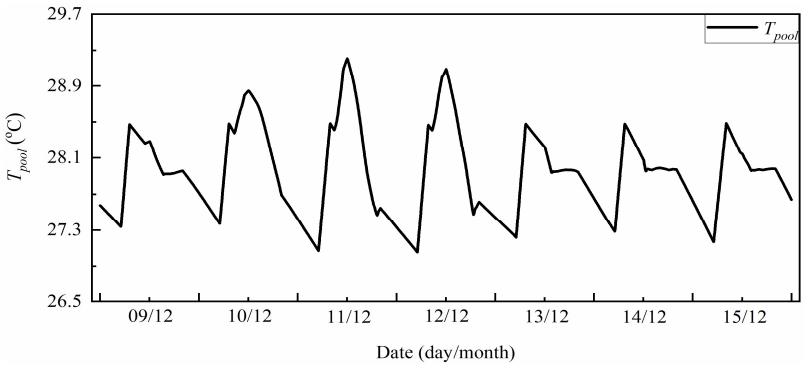

Fig. 13. Weekly water temperature variation of the pool.

6. Conclusions

An outdoor swimming pool heating system was developed and investigated in this study. The proposed system mainly consisted of solar collectors, air-source heat pumps, and PCM tank. Two important issues, including main components sizing and multi-criterion design were addressed. The important conclusions were presented as follows:

- The proposed heating system could efficiently reduce the CO_2 emission in comparison with a conventional electrical heating system. Case studies showed that the CO_2 emission reduction could be as high as 75.4% when compared with the conventional system.
- The proposed sizing strategy could give a reliable design if the worst-case weather condition was used. In Hong Kong, February 26th, 2005 could be chosen as the design day. Even if a middle-level design risk was utilized to identify the design value of the available solar energy intensity, the thermal comfort unmet percentage (TU) was still less than 7%.
- The design parameter (γ) that specified heat allocation to solar collectors and air-source heat pumps had a significant influence on the economic and energy performance of the proposed heating system. The multi-criterion design could balance different considerations in the aspects of both economic and energy performance.
- The proposed heating system could significantly reduce the total operating cost. Case studies showed that a suitable choice with $\gamma = 45\%$ (corresponding to the weighting factors for TU, IC, EC, and OC were set as 0.45, 0.25, 0.2, and 0.1, respectively), could lead to the average daily operating cost around HK$1,593 for a swimming pool with a standard size (50m×22m×1.785m).

Based on the above-mentioned points, it was concluded that the proposed heating system could find applications in outdoor swimming pools under subtropical climates.

Acknowledgment

The work described in this paper was supported by a grant from the Research Grants Council of the Hong Kong Special Administrative Region, China (Project No. 11208918) and a grant from Guangdong-Hong Kong Collaboration Scheme, China (Project No. 2017A050506058). The authors appreciated the support of the funding from Department of Energy and Process Engineering in Norwegian University of Science and Technology, Norway.

References

Abbas, Zafar, Ajay Kumar Tiwari, and Pradeep Kumar. 2018. *Emerging trends of plant physiology for sustainable crop production*: CRC Press.

Alkhamis, AI, and SA Sherif. 1992. "Performance analysis of a solar-assisted swimming pool heating system." Review of. *Energy* 17 (12):1165-72.

Bergman, Theodore L, and Frank P Incropera. 2011. *Fundamentals of heat and mass transfer*: John Wiley & Sons.

Brambley, MR, and SE Wells. 1983. "Energy-conservation measures for indoor swimming pools." Review of. *Energy* 8 (6):403-18.

Buonomano, Annamaria, Giuseppina De Luca, Rafal Damian Figaj, and Laura Vanoli. 2015. "Dynamic simulation and thermo-economic analysis of a PhotoVoltaic/Thermal collector heating system for an indoor–outdoor swimming pool." Review of. *Energy Conversion and Management* 99:176-92. doi: 10.1016/j.enconman.2015.04.022.

Chan, Wilco W, and Joseph C Lam. 2003. "Energy-saving supporting tourism sustainability: A case study of hotel swimming pool heat pump." Review of. *Journal of Sustainable Tourism* 11 (1):74-83.

Chow, T. T., Y. Bai, K. F. Fong, and Z. Lin. 2012. "Analysis of a solar assisted heat pump system for indoor swimming pool water and space heating." Review of. *Applied Energy* 100:309-17. doi: 10.1016/j.apenergy.2012.05.058.

Cover, Pool. "Cover Thickness." https://www.cultureindoor.eu/15080-ubbink-aqualiner-tarpaulin-for-pool-pvc-thickness-1mm-8x12m.html.

Croy, Reiner, and Felix A Peuser. 1994. "Experience with solar systems for heating swimming pools in Germany." Review of. *Solar Energy* 53 (1):47-52.

Dang, Aman. 1986. "A parametric study of swimming pool heating—I." Review of. *Energy Conversion and Management* 26 (1):27-31.

de Oliveira, Raphael Nunes, Ralney Nogueira Faria, Fernando Antonanzas-Torres, Luiz Machado, and Ricardo Nicolau Nassar Koury. 2015. "Dynamic model and experimental validation for a gas cooler of a CO2heat pump for heating residential water." Review of. *Science and Technology for the Built Environment* 22 (1):30-40. doi: 10.1080/23744731.2015.1070647.

Density, Water. 2020. "Water Density." Review of. doi: https://en.wikipedia.org/wiki/Density.

Govaer, David. 1984. "Determining the solar heating of swimming pools by the utilizability method." Review of. *Solar Energy* 32 (5):667-9.

Greyvenstein, Gideon P, and Josua P Meyer. 1991. "The viability of heat pumps for the heating of swimming pools in South Africa." Review of. *Energy* 16 (7):1031-7.

Haaf, Wilfried, Ulrich Luboschik, and Benno Tesche. 1994. "Solar swimming pool heating: description of a validated model." Review of. *Solar Energy* 53 (1):41-6.

Hahne, E, and R Kübler. 1994. "Monitoring and simulation of the thermal performance of solar heated outdoor swimming pools." Review of. *Solar Energy* 53 (1):9-19.

Harrington, Curtis, and Mark Modera. 2013. "Swimming pools as heat sinks for air conditioners: California feasibility analysis." Review of. *Energy and Buildings* 59:252-64. doi: 10.1016/j.enbuild.2012.12.038.

Hasan, Mushtaq I., Hadi O. Basher, and Ahmed O. Shdhan. 2018. "Experimental investigation of phase change materials for insulation of residential buildings." Review of. *Sustainable Cities and Society* 36:42-58. doi: 10.1016/j.scs.2017.10.009.

Heat. "Water specific heat." http://www.hk-phy.org/contextual/heat/tep/temch02_e.html.

Huang, Xingyi, and Chunyi Zhi. 2016. *Polymer Nanocomposites*: Springer.

Katsaprakakis, Dimitris Al. 2015. "Comparison of swimming pools alternative passive and active heating systems based on renewable energy sources in Southern Europe." Review of. *Energy* 81:738-53. doi: 10.1016/j.energy.2015.01.019.

Khaled, Nassim, and Bibin Pattel. 2018. *Practical Design and Application of Model Predictive Control: MPC for MATLAB® and Simulink® Users*: Butterworth-Heinemann.

Klein, SAea, A Beckman, W Mitchell, and A Duffie. 2011. "TRNSYS 17-A TRansient SYstems Simulation program." Review of. *Solar Energy Laboratory, University of Wisconsin, Madison*.

Kuyumcu, Muhammed Enes, Hakan Tutumlu, and Recep Yumrutaş. 2016. "Performance of a swimming pool heating system by utilizing waste energy rejected from an ice rink with an energy storage tank." Review of. *Energy Conversion and Management* 121:349-57. doi: 10.1016/j.enconman.2016.05.049.

Lam, Joseph C, and Wilco W Chan. 2001. "Life cycle energy cost analysis of heat pump application for hotel swimming pools." Review of. *Energy Conversion and Management* 42 (11):1299-306.

Li, W., M. C. Paul, N. Sellami, T. K. Mallick, and A. R. Knox. 2017. "Natural convective heat transfer in a walled CCPC with PV cell." Review of. *Case Studies in Thermal Engineering* 10:499-516. doi: 10.1016/j.csite.2017.10.009.

Li, Yantong, Zhixiong Ding, and Yaxing Du. 2020. "Techno-economic optimization of open-air swimming pool heating system with PCM storage tank for winter applications."

Review of. *Renewable Energy*.

Li, Yantong, Zhixiong Ding, Mohammad Shakerin, and Nan Zhang. 2020. "A multi-objective optimal design method for thermal energy storage systems with PCM: A case study for outdoor swimming pool heating application." Review of. *Journal of Energy Storage* 29. doi: 10.1016/j.est.2020.101371.

Li, Yantong, Gongsheng Huang, Huijun Wu, and Tao Xu. 2018. "Feasibility study of a PCM storage tank integrated heating system for outdoor swimming pools during the winter season." Review of. *Applied Thermal Engineering* 134:490-500. doi: 10.1016/j.applthermaleng.2018.02.030.

Li, Yantong, Gongsheng Huang, Tao Xu, Xiaoping Liu, and Huijun Wu. 2018. "Optimal design of PCM thermal storage tank and its application for winter available open-air swimming pool." Review of. *Applied Energy* 209:224-35. doi: 10.1016/j.apenergy.2017.10.095.

Li, Yantong, Nan Zhang, and Zhixiong Ding. 2020. "Investigation on the energy performance of using air-source heat pump to charge PCM storage tank." Review of. *Journal of Energy Storage* 28. doi: 10.1016/j.est.2020.101270.

Molineaux, Benoît, B Lachal, and O Guisan. 1994a. "Thermal analysis of five outdoor swimming pools heated by unglazed solar collectors." Review of. *Solar Energy* 53 (1):21-6.

Molineaux, Benoît, B Lachal, and Olivier Guisan. 1994b. "Thermal analysis of five unglazed solar collector systems for the heating of outdoor swimming pools." Review of. *Solar Energy* 53 (1):27-32.

Nord, Natasa, Live Holmedal Qvistgaard, and Guangyu Cao. 2016. "Identifying key design parameters of the integrated energy system for a residential Zero Emission Building in Norway." Review of. *Renewable Energy* 87:1076-87. doi: 10.1016/j.renene.2015.08.022.

Pirasaci, Tolga, and D. Yogi Goswami. 2016. "Influence of design on performance of a latent heat storage system for a direct steam generation power plant." Review of. *Applied Energy* 162:644-52. doi: 10.1016/j.apenergy.2015.10.105.

Plytaria, Maria T., Evangelos Bellos, Christos Tzivanidis, and Kimon A. Antonopoulos. 2019. "Financial and energetic evaluation of solar-assisted heat pump underfloor heating

systems with phase change materials." Review of. *Applied Thermal Engineering* 149:548-64. doi: 10.1016/j.applthermaleng.2018.12.075.

Rakopoulos, CD, and E Vazeos. 1987. "A model of the energy fluxes in a solar heated swimming pool and its experimental validation." Review of. *Energy Conversion and Management* 27 (2):189-95.

Ruiz, Elisa, and Pedro J. Martínez. 2010. "Analysis of an open-air swimming pool solar heating system by using an experimentally validated TRNSYS model." Review of. *Solar Energy* 84 (1):116-23. doi: 10.1016/j.solener.2009.10.015.

Shirazi, Ali, Sergio Pintaldi, Stephen D. White, Graham L. Morrison, Gary Rosengarten, and Robert A. Taylor. 2016. "Solar-assisted absorption air-conditioning systems in buildings: Control strategies and operational modes." Review of. *Applied Thermal Engineering* 92:246-60. doi: 10.1016/j.applthermaleng.2015.09.081.

Shirazi, Ali, Robert A. Taylor, Stephen D. White, and Graham L. Morrison. 2016. "Transient simulation and parametric study of solar-assisted heating and cooling absorption systems: An energetic, economic and environmental (3E) assessment." Review of. *Renewable Energy* 86:955-71. doi: 10.1016/j.renene.2015.09.014.

Somwanshi, Aneesh, Anil Kumar Tiwari, and Mahendra Singh Sodha. 2013. "Feasibility of earth heat storage for all weather conditioning of open swimming pool water." Review of. *Energy Conversion and Management* 68:89-95. doi: 10.1016/j.enconman.2012.12.024.

Sonnier, Rodolphe, Laurent Ferry, Benjamin Gallard, Abderrahim Boudenne, and François Lavaud. 2015. "Controlled Emissivity Coatings to Delay Ignition of Polyethylene." Review of. *Materials* 8 (10):6935-49. doi: 10.3390/ma8105349.

Stefan–Boltzmann. "Stefan–Boltzmann constant." https://en.wikipedia.org/wiki/Stefan%E2%80%93Boltzmann_constant.

Tank, Unit Cost of Water. "Unit Cost of Water Tank." https://www.alibaba.com/product-detail/Manufacturer-stainless-steel-water-storage-tank_1600056577337.html?spm=a2700.pc_countrysearch.main07.148.12a734cbrcoRDB.

Teodoriu, Gabriel, and Ion Serbanoiu. 2013. "Quantification of solar infrared radiation impact

on opaque surfaces of residential buildings envelope as heat gain factor for optimized energy balance model." Review of. *Buletinul Institutului Politehnic din lasi. Sectia Constructii, Arhitectura* 59 (3):55.

ThermoWorks. "water emissivity coefficient." https://www.thermoworks.com/emissivity-table.

Tian, Zhiyong, Bengt Perers, Simon Furbo, and Jianhua Fan. 2018. "Analysis and validation of a quasi-dynamic model for a solar collector field with flat plate collectors and parabolic trough collectors in series for district heating." Review of. *Energy* 142:130-8. doi: 10.1016/j.energy.2017.09.135.

Tian, Zhiyong, Shicong Zhang, Jie Deng, Jianhua Fan, Junpeng Huang, Weiqiang Kong, Bengt Perers, and Simon Furbo. 2019. "Large-scale solar district heating plants in Danish smart thermal grid: Developments and recent trends." Review of. *Energy Conversion and Management* 189:67-80. doi: 10.1016/j.enconman.2019.03.071.

ToolBox, Engineering. "Cover Emissivity Coefficient." https://www.engineeringtoolbox.com/emissivity-coefficients-d_447.html.

Vieira, Abel S., Rodney A. Stewart, and Cara D. Beal. 2015. "Air source heat pump water heaters in residential buildings in Australia: Identification of key performance parameters." Review of. *Energy and Buildings* 91:148-62. doi: 10.1016/j.enbuild.2015.01.041.

Watanabe, Takayuki, Hisashi Kikuchi, and Atsushi Kanzawa. 1993. "Enhancement of charging and discharging rates in a latent heat storage system by use of PCM with different melting temperatures." Review of. *Heat Recovery Systems and CHP* 13 (1):57-66.

Woolley, Jonathan, Curtis Harrington, and Mark Modera. 2011. "Swimming pools as heat sinks for air conditioners: Model design and experimental validation for natural thermal behavior of the pool." Review of. *Building and Environment* 46 (1):187-95. doi: 10.1016/j.buildenv.2010.07.014.

Yadav, YP, and GN Tiwari. 1987. "Analytical model of solar swimming pool: transient approach." Review of. *Energy Conversion and Management* 27 (1):49-54.

Yu, Xiaoling, Qian Lv, Lu Zhang, Xiaolin Wang, Xiangzhao Meng, and Zhenghua Zong. 2020. "Study of thermal performance of an air source heat pump heating for suburban residential buildings in Beijing." Review of. *Science and Technology for the Built*

Environment:1-14. doi: 10.1080/23744731.2020.1746152.

Zhao, J., J. I. Bilbao, E. D. Spooner, and A. B. Sproul. 2018. "Experimental study of a solar pool heating system under lower flow and low pump speed conditions." Review of. *Renewable Energy* 119:320-35. doi: 10.1016/j.renene.2017.12.006.

Zsembinszki, Gabriel, Mohammed M. Farid, and Luisa F. Cabeza. 2012. "Analysis of implementing phase change materials in open-air swimming pools." Review of. *Solar Energy* 86 (1):567-77. doi: 10.1016/j.solener.2011.10.028.